Hindawi
Wireless Communications and Mobile Computing
Volume 2022, Article ID 6964958, 9 pages
https://doi.org/10.1155/2022/6964958

Research Article

Full Scale Test and Numerical Simulation Based on Artificial Intelligence Background Analyze Hydraulic Structures and Derive Weir Height Equation

Xiuqin Cao and Guoyuan Hong

School of Environment and Energy Engineering, Beijing University of Civil Engineering and Architecture, Beijing 100044, China

Correspondence should be addressed to Guoyuan Hong; 201503020132@stu.bucea.edu.cn

Received 18 May 2022; Revised 9 June 2022; Accepted 10 June 2022; Published 25 June 2022

Academic Editor: Kalidoss Rajakani

The confluence overflow facility with transverse weir is adopted in China to reduce the occurrence of overflow. Under normal conditions, most of the facilities do not overflow. The study on the hydraulic structure without overflow is helpful to improve the pollutant interception efficiency. In addition, the weir height equation for different intercepting pipe diameters was required. Full scale experiments and simulation studies were carried out, and the reliability of the simulation results was verified by experiments. The simulation describes the hydraulic structure and shows that the backflow area appears on the side of the chamber away from the interceptor and at the inlet of the pipe. The results show that when the ratio of weir height to pipe diameter is less than 1.2, the closure pipe is non pressure closure, when the ratio is from 1.2 to 1.75, it becomes half pressure, and when the ratio is greater than 1.75, it is converted to pressure. The increased rate of intercepting flow with the rise of weir height would change under the effect of different flow characteristics. Based on the experimental data distribution and the hydraulic characteristic, the weir height equation was deduced for the pipe diameter of 0.4 m. Other pipe diameter simulations showed that this equation was also applicable.

1. Introduction

Combined sewer overflows (CSOs) generally contain a lot of pollutants, which have negative impacts on the receiving water body and aquatic ecosystems. Pollution loads in CSOs are mainly characterized by nutrients, organic compounds, heavy metals, and microorganisms [1–4]. Many other scholars are committed to the study of micro pollutants in CSO. The pollutant index of initial rainwater is higher than that of urban domestic sewage, but the composition is completely different from that of domestic sewageand and this part has been supplementedUrban water pollution caused by tire friction, brake pad friction, engine oil and detergent [5]. Due to the pollutant load, this practice can cause serious damage to the receptor water quality and effects on microbial diversity and even lead to restrictions in the use and destination of the receiving body. Converting combined sewer catchment to separate sewer catchments is a trend to solve the overflow pollution in China. However, the conversion will be limited by economy, transportation, culture, and other reasons. The transformation from confluence catchment to diversion catchment is beneficial to the environmental protection of the whole city, but it is very difficult to implement expensive and long construction period. To complete the project of this system, we must go through a transitional period of piecemeal and phased implementation and gradual improvement. Establishing CSO facilities on the existing combined pipe, using the original straight discharge pipe as the overflow pipe, and transporting contaminated water to the sewage treatment plant through the newly built intercepting pipe by a simple transverse weir is a treatment method.

Many researchers have studied and tested the weir discharge. Because the shape of the chamber is geometric and

different from the function of the interceptor, the weir discharge equation will be different from the standard weir. Marín et al. obtained a special equation in the transverse weir with complex chamber geometry [6]. The discharge coefficient of a side weir was reported by Fach et al. [7]. Valentine et al. suggested that a unique discharge formula exists in the oblique weir facility [8]. A tornado vortex is to be observed in front of the broad-crested weir when overflow [9]. However, few researches have been devoted to investigating un-overflow. The number of times overflows occur is controlled by the CSO facility, whether in China or other countries. This means that it is not weir discharge in most cases. The siltation was formed during this period. Thus, the hydraulic structure in the facility without overflow is required. As pointed out by Dufresne et al., a large nonsymmetrical circulation dominates the flow field in the chamber when the intercepting pipe and overflow channel are in one direction [10]. A multinomial flow to simulate the flow field distribution in the transverse weir facility showed that most particles settle in the chamber on the side away from the intercepting pipe [11]. At present, the research on the hydraulic structure is mainly concentrated in the chamber, and few works have been devoted to the study of the fluid properties of the intercepting pipe.

The setting of the weir height should also ensure that only overflows less than a certain frequency occur each year; that is, no weir discharge appeared under the design combined flow. Whether the weir can satisfy the needs of water environmental protection can be judged by the simulation of urban drainage system [12]. However, by studying the relationship between the weir height and the maximum intercepting flow (design combined flow) without overflow, a reasonable estimate of the weir height can easily be obtained. The number of repetitions of the urban drainage system simulation will be increased if the initial weir height value is not set to an appropriate value. Affected by local resistance, the weir height value will be small when it is calculated according to the uniform flow in open channel flow, and the overflow will occur in the design integrated flow. Ma and Dong claim that the intercepting pipe diameter and the weir height are the main factors affecting the maximum intercepting flow under the un-overflow [13]. A mathematical statement between the flow rate and weir height is established, which is suitable for determining the weir height value when the intercepting pipe diameter is between 0.3 m and 0.6 m (Table 1) [14]. With the increasing demand for water environmental protection, the diameter of intercepting pipe used in the actual project has arrived at 1.2 m in China. To attain the formula for weir height under the larger pipe is necessary.

Recognizing the hydraulic characteristics of weir CSO facility and deriving a unique equation of weir height from on-site experiments or lab tests on scaled or full-scale models are expensive. In terms of method, computational fluid dynamics (CFD) technology is more widely used in the simulation of hydraulic structures with significant flow characteristics. It has suitable numerical solutions for the flow characteristics of physical problems such as steady and unsteady flow, laminar flow, and turbulence and achieves the best in terms of calculation speed, stability, and accuracy, so as to reveal its comprehensive performance. Daal-Rombouts et al. combined lab experiments and field measurements to demonstrate that the complex hydraulic behavior, including a flow regime change, can be precisely simulated [15]. A similar conclusion is obtained by Dufresne et al. [10], who employed particle image velocimetry and acoustic Doppler velocimetry to measure the flow field, and compared to the simulated results.

Table 1: The weir height calculation formula in Chinese standard.

Intercepting pipe (m)	The weir height equation (1)
0.3	$h = (0.233 + 13 \bullet Q) \bullet d$
0.4	$h = (0.226 + 7 \bullet Q) \bullet d$
0.5	$h = (0.219 + 4 \bullet Q) \bullet d$
0.6	$h = (0.202 + 3 \bullet Q) \bullet d$

[1]In equations: h is weir height (m); d is intercepting pipe (m); Q is design intercepting flow (m^3/s).

This paper explores the hydraulic structure of the weir CSO facility, which contains the chamber and the intercepting pipe, and the reliable equation for weir height. Engineering experiments on a full-scale model and CFD simulation are used for this purpose. The engineering experiment will be devoted to determining the error of the weir height calculated by the uniform flow of the open channel and verifying the reliability of the CFD simulation. The simulation will work to sketch the hydraulic properties of the fluid. Combined with experiments and simulations, a reliable equation for weir height is deduced, and optimization suggestions will be obtained. The CFD is used to further simulate weir CSO facility with various intercepting pipe diameters to verify whether the calculation formula is applicable under different pipe diameters.

2. Materials and Methods

2.1. Engineering Experiment. A full-scale engineering experiment was studied to derive the weir height equation. According to the survey statistics, the intercepting pipe with a diameter of 0.4 m is the most widely used in China, so the pipe diameter is 0.4 m in the experiment. In the case where it does not overflow, the diameter of the combined pipe and the overflow pipe and the slope of all pipes are not the main factors affecting the intercepting flow [9]. The pipe diameters of the combined pipe and the overflow pipe are both taken as 1 m, and the slope of the pipes is 0.003. And all the tubes are made of concrete.

The experimental setup is shown in Figure 1. Pumps send clean water into a stilling tank, then which feeds on the weir chamber through an inflow conduit. An adjustable weir is fixed in the chamber. The liquid is firstly blocked by the weir without overflowing and returns to the water supply basin through the side intercepting pipe. With the rising of the upstream pumping flow, the excess fluid will pass over the weir into the overflow pipe and then into the

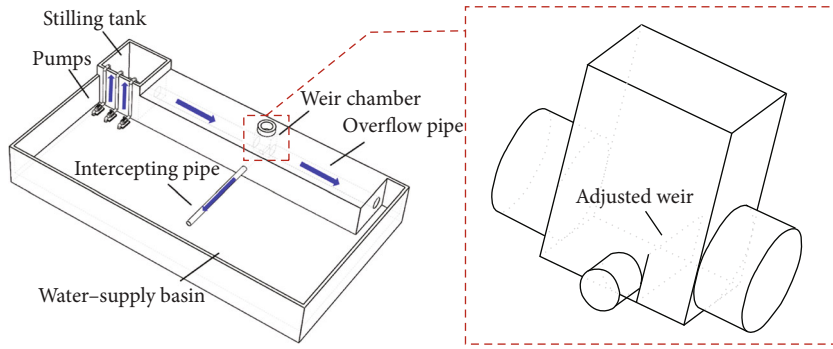

Figure 1: Schematic of the full-scaled experimental setup.

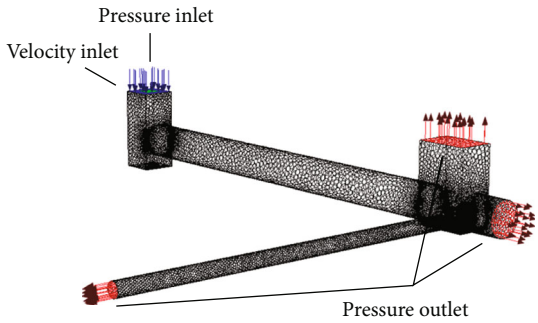

Figure 2: The meshing of the positive weir facility.

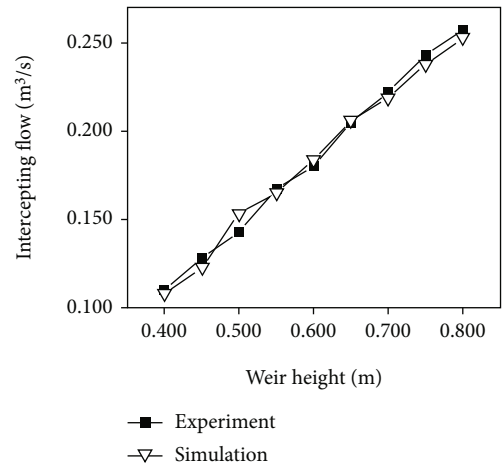

Figure 3: Error comparison between experimental and simulation results.

circulation. The physical model is instrumented with two flowmeters, one in the upstream pipe and the other in the side drain pipe.

2.2. Methods

2.2.1. Description of Methodology. Engineering experiment and simulation analysis are the two main methods of this research. The methodology is based on the following main steps:

(Step 1) Obtain flow data through full-scale engineering experiment, and compare errors of experiment and open channel calculation.

(Step 2) Construct geometric model and mesh, and set the numerical parameters to simulate using the FLUENT software, accounting for the initial and the boundary conditions. At last, accomplish simulations by convergence control.

(Step 3) Compare the simulation and experiment errors to verify the reliability of the modeling.

(Step 4) Analyze the hydraulic structure: streamline, velocity field, etc.

(Step 5) Derive the equation for the weir height through theoretical analysis and mathematical statistics.

(Step 6) Verify the equation based on experimental results.

(Step 7) Simulate facilities at other pipe diameters, and verify the applicability of the equation.

Engineering tests on full-scale under different intercepting pipe diameters are subject to time and economic constraints. The modeling method is proven to be reliable in Step 2 and Step 3. Therefore, the simulation result for the facilities with different drain pipe diameters can be considered is reliable.

2.2.2. Governing Equations and Turbulence Modeling. The continuity equation and Reynolds average Navier–Stokes equation were used for calculation [16], which could be expressed as

$$\frac{\partial \rho}{\partial t} + \frac{\partial}{\partial x_i}(\rho u_i) = 0, \tag{1}$$

$$\frac{\partial(\rho u_i)}{\partial t} + \frac{\partial}{\partial x_j}(\rho u_i u_j) = -\frac{\partial p}{\partial x_i} + \frac{\partial}{\partial x_j}\left(\mu \frac{\partial u_i}{\partial x_j} - \rho \overline{u_i}' u_j'\right) + S_b, \tag{2}$$

where ρ is density (kg·m^{-3}); t is time (s); i and j are 1, 2, and 3; x_i and x_j are coordinate components (m); u_i and u_j are the mean values of velocity in the i and j directions (m·s^{-1}); p is the mean value of pressure (Pa); μ is the dynamic viscosity of

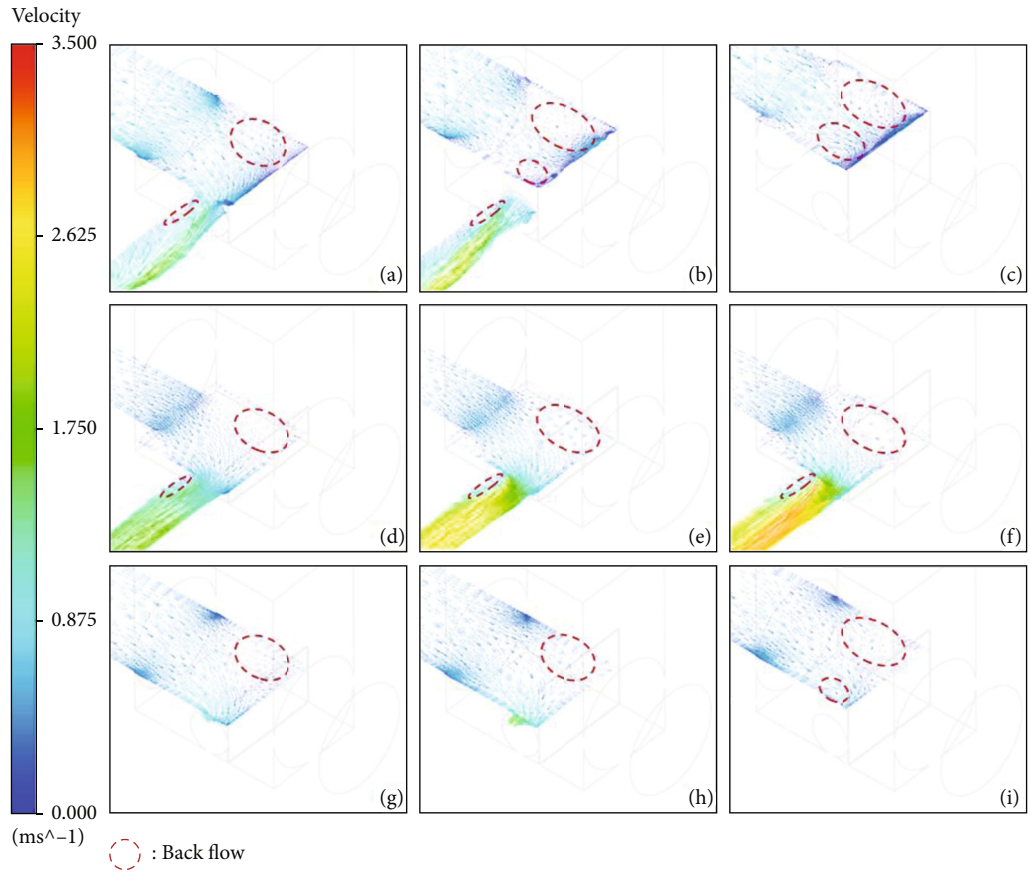

Figure 4: Velocity vector and back flow area in the weir CSO facility: (a) weir height $(h) = 0.4$ m, free face; (b) $h = 0.600$ m, free face; (c) $h = 0.800$ m, free face; (d) $h = 0.400$ m, horizontal plane height $(h_p) = 0.100$ m; (e) $h = 0.600$ m, $h_p = 0.100$ m; (f) $h = 0.800$ m, $h_p = 0.100$ m; (g) $h = 0.600$ m, $h_p = 0.400$ m; (h) $h = 0.800$ m, $h_p = 0.400$ m; (i) $h = 0.800$ m, $h_p = 0.600$ m.

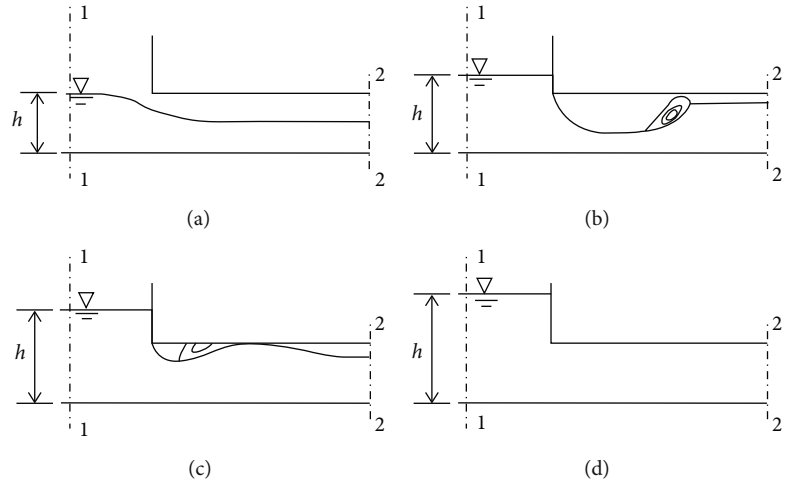

Figure 5: Three types of flow characteristics in intercepting pipes: (a) nonpressure; (b) semipressure I; (c) semipressure II; (d) pressure.

the fluid (Pa·s); S_b is the generalized source term of the momentum equation; and $\rho\bar{u}_i{}'u_j{}'$ is Reynolds stress.

The Shear Stress Transport (SST) turbulence model combines the advantages of both the standard k-ε and the k-ω turbulence model [17]. In many studies, the results simulated using the SST model has produced reliable results [18]. Therefore, the SST was applied in the viscous model.

2.2.3. Geometry and Computational Cells. Taking the intercepting pipe of 0.4 m and the weir height of 0.4 m as an example, the geometry of the facility is perfectly set in the

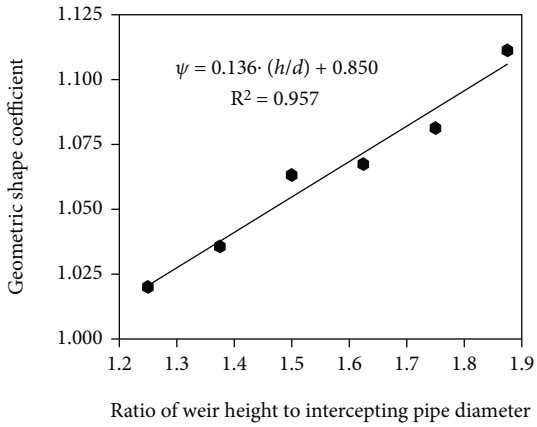

Figure 6: Relationship between geometric shape coefficient (ψ) and the ratio of weir height to the intercepting pipe diameter.

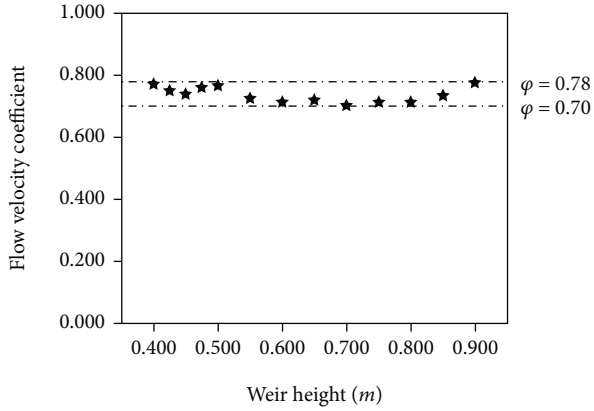

Figure 7: Flow velocity coefficient (φ).

Gambit code. Meshing is based on the Mosaic Poly-Hexcore (Figure 2). The greater the number of cells in the mesh grid, the more accurate will be the results, but the consumption of computing resources increases drastically with mesh density. 520,000 grids were selected to strike a balance between the quality of results and calculate consumption. Figure 3 shows that the simulation results agreed well with the experimental data, and the maximum error of the combined flow is 7.14%, which is within a reasonable range.

2.2.4. Boundary Conditions. Three boundary conditions are used for our study: velocity-inlet, pressure-outlet, and roughness. The flow is injected to obtain the condition just before an overflow occurs by constantly adjusting the inlet velocity. The roughness condition is used to the assessment of the wall functions that is set as 0.3 mm with the fluid in engineering test is clean water. In the liquid phase, the value of the volume fraction is imposed to be equal to 1. On the contrary, it is 0 in the air phase.

3. Results and Discussion

3.1. Hydraulic Structure in Chamber. Analyze hydraulic movement in the chamber. The weir blocking will cause backflow to occur [10]. The velocity in the backflow area is slow, and the particulate matter carried in the combined sewage will be prone to sedimentation. Sediments are easily washed away under high flow and can cause pollution if spilled into the river. Figure 4 shows the velocity vector of the free face and horizontal direction. An asymmetric circulation appears on the free surface at a weir height of 0.800 m (Figure 4(c)). The phenomenon is consistent with Dufresne et al. [10]. The gap between the sizes of the asymmetrical circulations becomes larger due to the influence of the lateral discharge when the horizontal plane height is 0.600 m (Figure 4(f)). Only unilateral recirculation occurs when the horizontal plane heights are 0.100 m and 0.400 m (Figures 4(h) and 4(i)). A similar phenomenon can also be observed when the weir heights are 0.400 m (Figures 4(a) and 4(d)) and 0.600 m (Figures 4(b), 4(e), and 4(g)). In summary, there is a backflow before the weir on the side far from the intercepting pipe, no matter at the top or the bottom, wherefore the place is silt prone point. The siltation of this part can be effectively reduced by setting the guide wall and decreasing the corner of the intercepting pipe.

The blockage of the weir and the reduction of the flow cross-section at the inlet of the intercepting pipe will cause the water level in the chamber to be high, which is the main factor for low weir height calculated by the open channel.

3.2. Hydraulic Structure in Intercepting Pipe. The hydraulic behavior within the intercepting pipe also has a significant impact on the intercepting capability just before spill flow occurs. The liquid in the chamber close to the sidewall of the drain duct flows to the inlet of the tube and then is forced to leave the wall due to the bent flow, and the boundary layer separation would be occurred [19]. After the liquid enters the tube, it will flow to the void by the separation of the boundary layer, thereby forming a backflow (Figure 4). The return zone will inhibit the liquid from entering the tube. The return zone shrinks as the angle of the flow turns smaller [20]. Therefore, reducing the angle between the interception pipe and the water flow direction in the combined pipe can improve the intercepting capacity. The recirculation at the inlet of the intercepting pipe will also easily form siltation, but the settled particles here will eventually enter the sewage plant after being washed, which has a little impact on the water environment.

When the weir height is less than or equal to 0.600 m (Figures 4(a), 4(b)), the intercepting pipe is the partially filled flow. This is because the water is narrowed by the shrink of the flow cross-section, and the water level in the intercepting pipe is lower than that in the chamber. In addition, the shift of potential energy to kinetic energy will occur during lateral discharge, which will also cause the water level to fall in the intercepting pipe. It becomes full flow until the weir height increases to 0.800 m (Figure 4(c)).

With the weir height rise, the intercepting pipe can be divided into nonpressure, semipressure, and pressure (Figure 5). It is nonpressure when the weir height is the same as the tube diameter. The water flow phenomenon at the inlet of the nonpressure intercepting pipe is similar to the

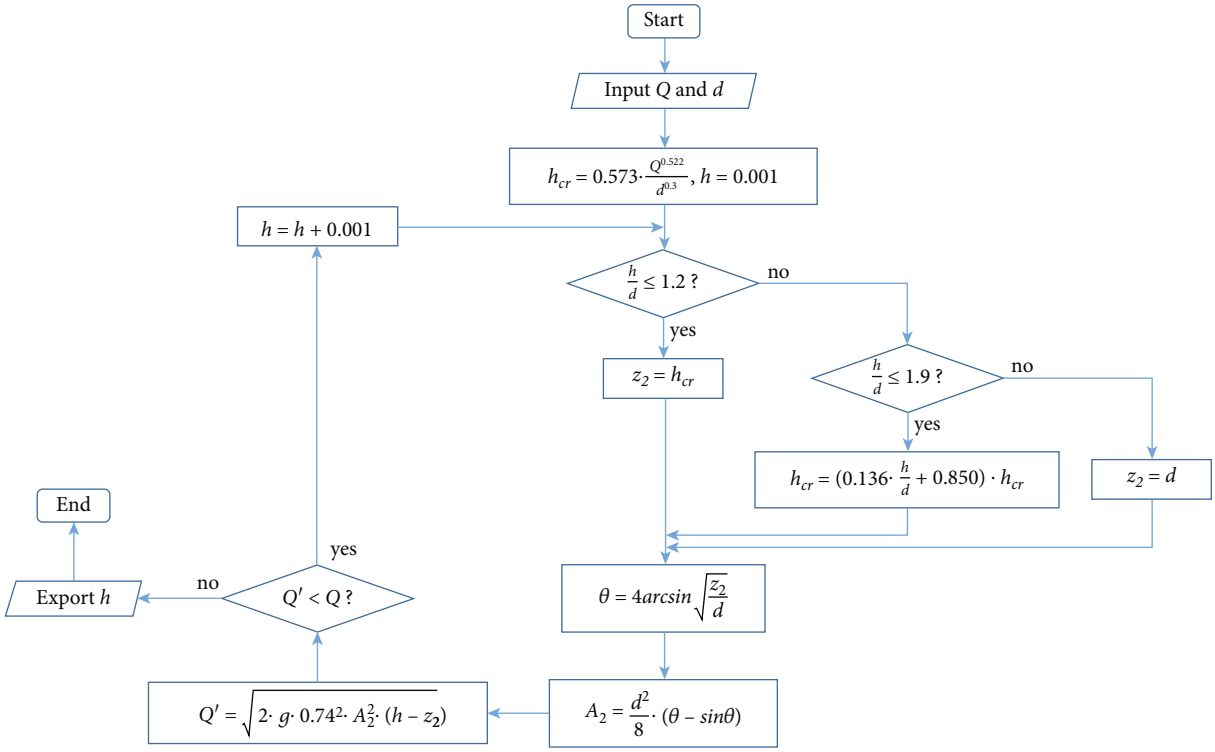

Figure 8: Weir height iterative calculation program.

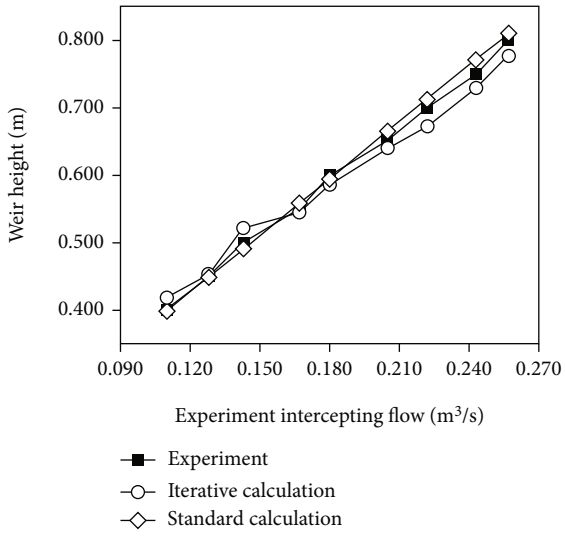

Figure 9: The error between experiment and calculation with the intercepting pipe diameter is 0.4 m.

broad-crested weir flow. That is, the water flow does not in contact with the top of the side drain pipe over the entire length of the conduit, and the pressure at each point on the water surface is equal to the atmospheric pressure (Figure 5(a)). The flow contacts the top at the inlet of the intercepting pipe with the weir gradually rising, and the pipe becomes a semipressure type. The semipressure type resembles outflow under gates. There is a minimum vena contract upstream of the pipe, and its water depth is less than the critical depth. The conversion of kinetic energy to potential energy downstream causes the lower reaches a level to be higher than the critical depth. The hydraulic jump will be happened due to the height difference between the upstream and downstream. Only a small part of the inlet is pressure, and the rest are free surface when the nonpressure exactly converts to the semipressure (Figure 5(b)). The water level increment resulting from the transformation of potential energy will enhance with the rise of the weir height. A negative pressure zone may appear in the area before the hydraulic jump when the increment is limited by the tube diameter (Figure 5(c)). Besides, the position of the hydraulic jump will also move to the inlet with the increase of the weir. In the pressure stage, the water is in contact with the top of the pipe over the entire length and has no free surface (Figure 5(d)). The transformation of water flow characteristics will change the rate of intercepting flow increasing with the increase of weir height. The rate is the fastest when the pipe is in the pressure, second in the semipressure, and slowest in the nonpressure.

3.3. Formulation for Weir Height. Select the flow cross-section 1-1 in the chamber and the flow section 2-2 at the outlet of the intercepting branch (Figure 5), and establish the Bernoulli equation as follows:

$$z_1 + \frac{\alpha_1 v_1^2}{2g} + \frac{p_1}{\rho g} = z_2 + \frac{\alpha_2 v_2^2}{2g} + \frac{p_2}{\rho g} + h_w, \tag{3}$$

where z is the elevation head, α is the kinetic energy correction factor, v is velocity, g is the gravitational acceleration, p is the pressure, ρ is the fluid density, and h_w is head loss.

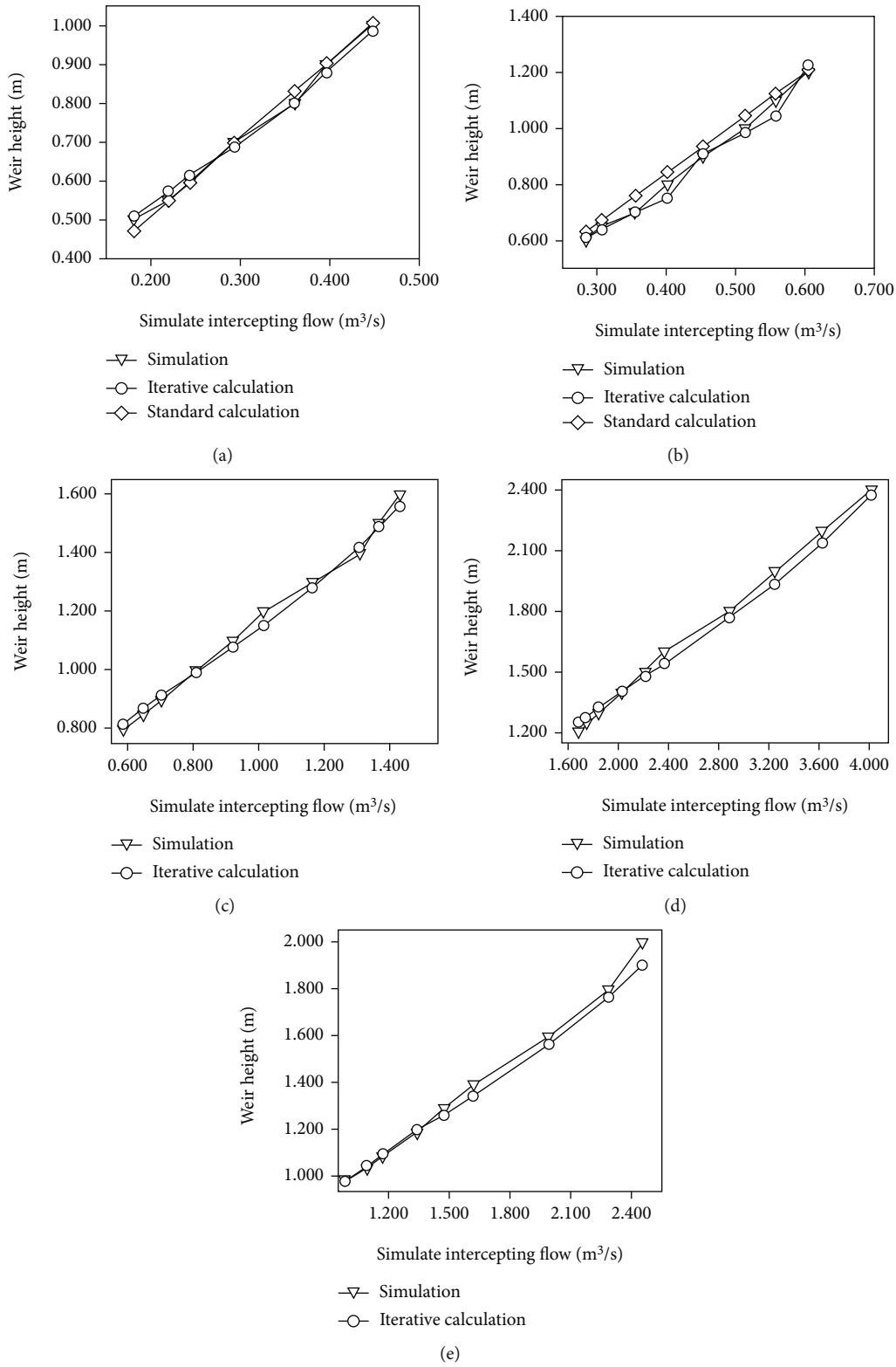

Figure 10: Error between simulation and calculation with the different intercepting pipe diameter (d): (a) $d = 0.5$ m; (b) $d = 0.6$ m; (c) $d = 0.8$ m; (d) $d = 1.0$ m; (e) $d = 1.2$ m.

Obviously, z_1 equals h (the weir height), and α is usually taken 1 in engineering. It can be considered that p_1 and p_2 are equal to atmospheric pressure because the intercepting pipe is generally free outflow when the un-overflow. The blocking of the weir and the diversion of the water flow make v_1 smaller than v_2, which can be observed in

Figure 4. Therefore, the effect of the traveling head can be ignored. Since the length of the branch pipe is generally short, the influence of the drag losses can also be ignored; then h_w is local loss:

$$h_w = \xi \bullet \frac{V_2^2}{2g}, \tag{4}$$

where ξ is the local drag coefficient. The flow equation can be expressed as:

$$Q = v_2 A_2, \tag{5}$$

where Q is flow rate and A is the area of flow cross-section. Then, h can be expressed as

$$h = \frac{Q^2}{2g\varphi^2 A_2^2} + z_2, \tag{6}$$

where φ is flow velocity coefficient with $\varphi = 1/\sqrt{(1+\xi)}$. A_2 can be counted by the following: $A_2 = d^2/8 \bullet (\theta - \sin\theta)$

$$\begin{aligned} A_2 &= \frac{d^2}{8} \bullet (\theta - \sin\theta), \\ \theta &= 4 \arcsin\sqrt{\frac{z_2}{d}}, \end{aligned} \tag{7}$$

where θ is the central angle of the flow cross-section of the intercepting pipe. Li [21] suggested an explicit equation for critical depth (h_{cr}) in a circular section tunnel:

$$h_{cr} = 0.573 \bullet \frac{Q^{0.522}}{d^{0.3}}. \tag{8}$$

The simulation results indicated that the hydraulic characteristics in the corresponding intercepting pipe can be divided into three layers: nonpressure ($h/d \le 1.2$), semipressure ($1.2 < h/d \le 1.75$), and pressure ($h/d > 1.75$). The simulation results show that z_2 is greater than or equal to d when there is no pressure and are equal to d. Assuming the semipressure conforms to $z_2 = \psi h_{cr}$, where ψ is the geometric shape coefficient, which is related to the h and d. According to the dimensionless criterion, the mathematical-statistical analysis of ψ and h/d is based on the dimensionless principle in Figure 6. There is a significant linear relationship between ψ and h/d ($R^2 = 0.957$). Thence, the equation for z_2 expression is obtained:

$$\begin{cases} z_2 = h_{cr}\dfrac{h}{d}1.2, \\ z_2 = d\dfrac{h}{d} > 1.75, \\ z_2 = \psi h_{cr} = \left(0.136 \bullet \dfrac{h}{d} + 0.850\right) \bullet h_{cr} 1.2 < \dfrac{h}{d} \le 1.75. \end{cases} \tag{9}$$

In particular, since different hydraulic characteristics are divided into estimation intervals, the calculated z_2 may be greater than d when h/d is close to 1.9, and $z_2 = d$ is taken at this time. After that, calculate φ with different h and d (Figure 7). The value of φ is between 0.70 and 0.78. Take φ as 0.74 for simplifying the calculation.

So far, h just un-overflow can be obtained by iterative calculations under different design Q and different d through the aforementioned equations. Figure 8 shows the iterative calculation program for h.

The errors among the iterative calculation result, the standard calculation (Table 1), and the lab tests on full-scale are shown in Figure 9. The errors are less than 5%, and the iterative calculation result is reliable. Figure 10 shows the comparison between the simulation results and the iterative calculation results under different intercepting pipe diameters. Their maximum error is also within 5%, indicating that the iterative calculation method of the weir height can be applied to the CSO facilities with different interception pipe diameters.

4. Conclusions

On the basis of experimental data and simulation, this paper discusses the horizontal weir combined sewer overflow device and discusses the hydraulic structure of weir CSO facilities, including chamber and interceptor, as well as the reliable equation and optimization suggestion of weir height. The hydraulic structure simulation analysis showed that the backflow area appeared at the side of the chamber away from the pipe and at the inlet of the pipe, due to the action of the weir and the lateral discharge pipe. The backwater effect can be effectively reduced by setting the guide wall and reducing the corner of the intercepting pipe.

Analyzing flow characteristics in the intercepting pipe, the intercepting pipe can be divided into nonpressure, semipressure, and pressure when the weir height and the pipe diameter ratio are less than 1.2, from 1.2 to 1.9, and greater than 1.9. The growth rate of intercepting flow becomes faster with the rise of weir height under the action of pressure.

On account of the division within the intercepting pipe and the experimental data and mathematical theoretical analysis, the weir height equation under no overflow when the intercepting pipe diameter is equal to 0.4 m is obtained. The results show that the weir height equation can adapt to other pipe diameters, simplify the design process of weir CSO facilities, and improve efficiency and accuracy. And this equation is also applicable to the calculation of weir height in engineering and the appropriate estimation of urban drainage system simulation, which can simplify this process.

Data Availability

The data underlying the results presented in the study are available within the manuscript.

Conflicts of Interest

The authors declare no conflict of interest.

Authors' Contributions

X-QC and G-YH did the conceptualization and writing—review and editing. G-YH is assigned to the methodology, software, validation, formal analysis, data curation, writing—original draft preparation, and visualization. X-QC is responsible for the resources, supervision, project administration, and funding acquisition. All authors have read and agreed to the published version of the manuscript.

Acknowledgments

This research was funded by the China Association for Engineering Construction Standardization that prepares the funded project (technical specification for intercepting facility of combined sewage system). Thanks are due to Beijing Drainage Group Co. Ltd. for the assistance with the experiments.

References

[1] L. Barone, M. Pilotti, G. Valerio et al., "Analysis of the residual nutrient load from a combined sewer system in a watershed of a deep Italian lake," *Journal of Hydrology*, vol. 571, pp. 202–213, 2019.

[2] Z. X. Xu, J. Wu, H. Z. Li et al., "Characterizing heavy metals in combined sewer overflows and its influence on microbial diversity," *Sci Total Environ.*, vol. 625, pp. 1272–1282, 2018.

[3] M. A. Aukidy and P. Verlicchi, "Contributions of combined sewer overflows and treated effluents to the bacterial load released into a coastal area," *Sci Total Environ.*, vol. 607, pp. 483–496, 2017.

[4] G. D. Marinis, "Microplastics in combined sewer overflows: an experimental study," *J Mar Sci Eng.*, vol. 9, p. 1415, 2021.

[5] M. A. Launay, U. Dittmer, and H. Steinmetz, "Organic micropollutants discharged by combined sewer overflows - characterisation of pollutant sources and stormwater-related processes," *Water Research*, vol. 104, pp. 82–92, 2018.

[6] A. M. Marín, N. Rivière, and G. L. Kouyi, "DSM-flux: a new technology for reliable combined sewer overflow discharge monitoring with low uncertainties," *Journal of Environmental Management*, vol. 215, pp. 273–282, 2018.

[7] S. Fach, R. Sitzenfrei, and W. Rauch, "Determining the spill flow discharge of combined sewer overflows using rating curves based on computational fluid dynamics instead of the standard weir equation," *Water Science and Technology*, vol. 60, no. 12, pp. 3035–3043, 2009.

[8] E. Valentine, K. Kronebusch, D. Z. Zhu et al., "Combined sewer overflow over an oblique weir at Rat Creek in Edmonton, Alberta," *Canadian Journal of Civil Engineering*, vol. 37, no. 3, pp. 477–488, 2010.

[9] Z. Zachoval and L. Roušar, "Flow structure in front of the broad-crested weir," *Epj Web of Conferences.*, vol. 92, p. 02117, 2015.

[10] M. Dufresne, J. Vazquez, A. Terfous, A. Ghenaim, and J. Poulet, *Three-Dimensional Flow Measurements and CFD Modelling in a Storm-Water Tank*, International Conference on Sustainable Techniques & Strategies in Urban Water Management, Lyon, France, June, 2007.

[11] J. F. Lei, "Three-dimensional simulation calculation of overflow weir well with Fluent software," in *Master, College of Civil Engineering*, Tongji University, Shanghai, 2005.

[12] Z. Wei, H. Shangguan, J. Zhan et al., "Water quality-based double-gates control strategy for combined sewer overflows pollution control," *Watermark*, vol. 13, no. 4, p. 529, 2021.

[13] J. L. Ma and S. X. Dong, "Study on the performance of sewage interception in rainwater overflow well in combined pipeline," *J BEIJING U Civil Eng Archit.*, vol. 2, pp. 72–80, 1990, (In Chinese).

[14] Ministry of Health of the People's Republic of China, Standardization Administration, *Standards for Design of Outdoor Wastewater Engineering (GB 50014-2021)*, Standards Press of China, Beijing, 2021.

[15] P. V. Daal-Rombouts, A. Tralli, F. Verhaart, J. Langeveld, and F. Clemens, "Validation of computational fluid dynamics for deriving weir discharge relationships with scale model experiments and prototype measurements," *Flow Measurement and Instrumentation*, vol. 58, pp. 52–61, 2017.

[16] F. Li, Y. Li, X. Sun, and X. Yang, "Numerical simulation of flow velocity characteristics during capsule hydraulic transportation in a horizontal pipe," *Watermark*, vol. 12, no. 4, p. 1015, 2020.

[17] M. S. Akoz, V. Gumus, and M. S. Kirkgoz, "Numerical simulation of flow over a semicylinder weir," *Journal of Irrigation and Drainage Engineering*, vol. 140, pp. 14–16, 2014.

[18] M. S. Kirkgoz, M. S. Akoz, and A. A. Oner, "Experimental and theoretical analyses of two-dimensional flows upstream of broadcrested weirs," *Canadian Journal of Civil Engineering*, vol. 35, no. 9, pp. 975–986, 2008.

[19] R. Venters, B. T. Helenbrook, G. Ahmadi, D. Bohl, and A. Bluestein, "Flow through an elbow: a direct numerical simulation investigating turbulent flow quantities," *Int J Heat Fluid FL.*, vol. 90, article 108835, 2021.

[20] Q. Hou, A. C. H. Kruisbrink, F. R. Pearce, A. S. Tijsseling, and T. Yue, "Smoothed particle hydrodynamics simulations of flow separation at bends," *Computers and Fluids*, vol. 90, pp. 138–146, 2014.

[21] W. Li, *Handbook of Hydraulic Calculations*, China Water & Power Press, Beijing, China, 2rd ed. edition, 2006, (In Chinese).